International Journal of Pharmaceutics 415 (2011) 284–292

Contents lists available at ScienceDirect

International Journal of Pharmaceutics

journal homepage: www.elsevier.com/locate/ijpharm

Pharmaceutical Nanotechnology

Brain delivery and cellular internalization mechanisms for transferrin conjugated biodegradable polymersomes

Zhiqing Pang[a,b], Huile Gao[a,b], Yuan Yu[c], Jun Chen[a,b], Liangran Guo[a,b], Jinfeng Ren[a,b], Ziyi Wen[a,b], Jinghan Su[a,b], Xinguo Jiang[a,b,c,*]

[a] Department of Pharmaceutics, School of Pharmacy, Fudan University, Shanghai 201203, People's Republic of China
[b] Key Laboratory of Smart Drug Delivery, Ministry of Education & PLA, 201203, People's Republic of China
[c] Department of Pharmaceutics, School of Pharmacy, The Second Military Medical University, Shanghai 200433, People's Republic of China

ARTICLE INFO

Article history:
Received 1 March 2011
Received in revised form 23 April 2011
Accepted 24 May 2011
Available online 30 May 2011

Keywords:
Biodegradable polymersomes
Transferrin
Brain delivery
Cellular internalization
Brain–blood barrier (BBB)

ABSTRACT

Transferrin conjugated biodegradable polymersomes (Tf-PO) were exploited for efficient brain drug delivery, and its cellular internalization mechanisms were investigated. Tf-PO was prepared by a nano-precipitation method with an average diameter of approximately 100 nm and a surface Tf molecule number per polymersome of approximately 35. It was demonstrated that the uptake of Tf-PO by bEnd.3 was mainly through a clathrin mediated energy-dependent endocytosis. Both the Golgi apparatus and lysosomes are involved in intracellular transport of Tf-PO. Thirty minutes after a 50 mg/kg dose of Tf-PO or PO was injected into rats via the tail vein, fluorescent microscopy of brain coronal sections showed a higher accumulation of Tf-PO than PO in the cerebral cortex, the periventricular region of the lateral ventricle and the third ventricle. The brain delivery results proved that the blood–brain barrier (BBB) permeability surface area product (PS) and the percentage of injected dose per gram of brain (%ID/g brain) for Tf-PO were increased to 2.8-fold and 2.3-fold, respectively, as compared with those for PO. These results indicate that Tf-PO is a promising brain delivery carrier.

1. Introduction

Due to the blood–brain barrier (BBB), which prevents most drugs from entering the brain, the prognosis for many neurological disorders remains poor, and targeting drug delivery to the brain is still a therapeutic challenge (Pardridge, 2002, 2007). Over the last decade, an increasing number of studies have been performed to develop strategies for effective brain drug delivery and nanocarrier systems such as micelles (Liu et al., 2008), liposomes (Ying et al., 2009), nanoparticles (NPs) (Gan and Feng, 2010), dendrimers (Ke et al., 2009), and polymersomes (Pang et al., 2008) have emerged as interesting treatment strategies. Among the various nanocarriers, polymersomes currently attract great interest as promising alternatives to liposomes regarding their remarkable and feasible characteristics such as stealthiness, improved stability, and ease of functionalization (Discher and Eisenberg, 2002; Discher et al., 2007; Du and O'Reilly, 2009). In addition, polymersomes can be designed to combine and optimize features required for drug delivery applications, such as biodegradability (Liu et al., 2010; Meng et al., 2003), targeting capability (Zhou et al., 2006), and responsiveness to biologically relevant stimuli (Meng et al., 2009) such as pH (Chen et al., 2010), temperature (Qin et al., 2006), light (Mabrouk et al., 2009), and a reductive environment (Cerritelli et al., 2007). Therefore, polymersomes are good candidate carriers for brain drug delivery; however, the application of biodegradable polymersomes as brain drug delivery systems in vivo has little been reported.

Similar to many drugs, nanocarriers are not able to breach the BBB. Thus, to enable the nanocarriers to cross the BBB, target ligands are attached to the surface of the nanocarriers to target the nanocarriers to receptors on the BBB, thus facilitating receptor-mediated transcytosis of the nanocarriers. The specific receptors on the BBB used for brain delivery usually include the transferrin receptor (TfR), the insulin receptor, the low-density lipoprotein receptor family, the diphtheria toxin receptor, and the leptin receptor (de Boer et al., 2003). Among these receptors, TfR, a transmembrane glycoprotein, consisting of two linked 90-kDa subunits, is the most widely studied receptor for BBB targeting (Qian et al., 2002). The receptor is highly expressed by brain capillaries to mediate the delivery of iron to the brain (Jefferies et al., 1984) and is also expressed by neurons (Jones and Shusta, 2007). Moreover, the level of TfR expression in other normal, non-dividing healthy tissues is nearly undetectable (Gatter et al., 1983). Therefore, a single ligand targeted to TfR can not only mediate the transport of nanocarriers across the BBB but can also help to increase intracellular delivery

* Corresponding author at: Department of Pharmaceutics, School of Pharmacy, Fudan University (Zhangjiang Campus), 826 Zhangheng Road, Shanghai 201203, People's Republic of China. Tel.: +86 21 5198 0067; fax: +86 21 5198 0069.
E-mail address: xgjiang@shmu.edu.cn (X. Jiang).

0378-5173/$ – see front matter © 2011 Elsevier B.V. All rights reserved.
doi:10.1016/j.ijpharm.2011.05.063

into neurons (Jones and Shusta, 2007). As a classic BBB targeting ligand, holo-transferrin has a high affinity for the TfR and has been successfully used for brain delivery of nanocarriers (Gan and Feng, 2010; Gupta et al., 2007; Qian et al., 2002; Ren et al., 2010) even though high levels of endogenous transferrin nearly saturate transferrin receptors (de Boer and Gaillard, 2007). Thus, transferrin has been shown to be a promising ligand for targeted drug delivery to the brain.

Although many studies have demonstrated that transferrin increases brain delivery of nanocarriers in vitro and in vivo, the brain uptake mechanisms of transferrin modified nanocarriers have not yet been clearly defined. Hence, the main aims of this study were to develop biodegradable polymersomes that are functionalized with transferrin (Tf-PO) for brain delivery and to elucidate their cellular internalization mechanisms. Biodegradable poly(ethyleneglycol)–poly(ε-caprolactone) (PEG–PCL) was applied to prepare polymersomes by a nanoprecipitation method. The morphology and particle size of Tf-PO were characterized by transmission electron micrograph and dynamic light scattering. Using coumarin-6 as a fluorescent probe, the cellular uptake mechanisms and brain delivery of Tf-PO were investigated. A cell viability assay was also performed to confirm the safety of the biodegradable Tf-PO.

2. Materials and methods

2.1. Materials and animals

Monomethoxy-polyethyleneglycol (MPEG, Mn = 3000 Da) and hydroxy-polyethyleneglycol-maleimide (Maleimide-PEG, Mn = 3400 Da) were purchased from PegBio Corporation (Suzhou, China) and Laysan Bio (Arab, AL, USA), respectively. ε-Caprolactone (ε-CL) was ordered from Dow (Houston, TX, USA). Stannous octoate (95% pure), holo-transferrin, monensin, Brefeldin A, and 2-iminothiolane (Traut's reagent) were purchased from Sigma (Saint Louis, MO, USA). Coumarin-6 and coumarin-7 were from Aldrich. A human transferrin ELISA quantitation kit was obtained from Bethyl (Montgomery, TX, USA). The BCA protein assay was from Shanghai Shenergy Biocolor Bioscience and Technology Corporation (China). Filipin was purchased from Fluka (Germany). Chlorpromazine was kindly provided by Shanghai Mental Health Center. The bEnd.3 cell line was from the American Type Culture Collection (Rockville, MD). Fetal bovine serum and related cell culture medium were from Invitrogen (Gibco, Carlsbad, CA). Plastic cell culture dishes, plates, and flasks were ordered from Corning Incorporation (Lowell, MA). Double distilled water was purified using a Millipore Simplicity System (Millipore, Bedford, MA, USA). All the other chemicals were analytical reagent grades and were used without further purification.

Sprague-Dawley rats (weighing 200–230 g) were obtained from Shanghai SLAC Laboratory Animal Co. Ltd. (Shanghai, China). The animals used for the experiment were treated according to protocols that had been evaluated and approved by the ethical committee of Fudan University.

2.2. Preparation and characterization of transferrin conjugated polymersomes

2.2.1. Copolymer synthesis and characterization

The MPEG–PCL or Maleimide-PEG–PCL diblock copolymers were synthesized by ring-opening polymerization of ε-CL using MPEG or Maleimide-PEG–PCL as the initiator (Pang et al., 2008). ^{1}H NMR spectra of these copolymers were recorded in $CDCl_3$ with a Varian Mercury Plus-400 MHz apparatus. Chemical shifts in ppm (δ) were determined, and the chloroform signals at 7.26 ppm were used as references. The integrals of the peaks corresponding to the PCL methylene protons (δ 2.31 ppm) and the PEG methylene protons (δ 3.65 ppm) were used to calculate the average number molecular weight (Mn) of the PCL block (He et al., 2004). The peak at 6.70 ppm for the maleimide protons was used to validate the preservation of the maleimide function in the synthesized Maleimide-PEG–PCL. Molecular weight and molecular distribution were also determined by gel permeation chromatography (GPC) with an Angilent 1100 GPC (Angilent, USA), using tetrahydrofuran (THF) as the solvent.

2.2.2. Preparation of biodegradable polymersomes conjugated with transferrin

Biodegradable polymersomes were made with a blend of MPEG–PCL and Maleimide-PEG–PCL by a nanoprecipitation method (Meng et al., 2005). In brief, 20 mg of MPEG–PCL and 2 mg of Maleimide-PEG–PCL were dissolved in 1.0 mL of THF and were then injected slowly into 10 mL of 0.01 M PBS (pH 7.4). Mild stirring was performed to induce self-assembly for 30 min. The polymersomes solution was dialyzed against 0.01 M PBS (pH 7.4) to remove THF and was followed by concentration of the solution using a TM Ultra-4 (Amicon) concentrator tube. For Tf conjugation, Tf was thiolated and characterized in the same manner as our previous work (Lu et al., 2005b). Thiolated Tf was then incubated for 8 h with the above concentrated polymersomes with a thiol group to maleimide group molar ratio of 1:3. The resulting Tf-PO was purified by passing it through a Sepharose CL-4B column, and it was eluted with 0.01 M PBS buffer (pH 7.4).

The preparation of polymersomes loaded with coumarin-6 was the same as that of blank Tf-PO, except that an additional 120 μg of coumarin-6 was added to the copolymer solution.

2.2.3. Morphology, particle size and zeta potential

The formation of blank polymersomes was visualized by Cryo-transmission electron micrograph (Cryo-TEM, JEOL 2010, Japan) (Bermudez et al., 2002). Tf-PO was observed by transmission electron microscope (TEM, JEM-1230, JEOL, Japan) following negative staining with 1% uranyl acetate solution. The mean diameters and zeta potential of Tf-PO were determined by dynamic light scattering (DLS) using a Zeta Potential/Particle Sizer NICOMP TM 380 ZLS (S.NICOMP PARTICLE SIZE SYSTEM, Santa Barbara, USA). Surface Tf densities were determined by the ELISA method combined with a turbidimetry method, as previously described (Pang et al., 2008).

2.2.4. Drug loading efficiency and in vitro release of coumarin-6 from Tf-PO

The drug loading efficiency (DLE) of coumarin-6 in Tf-PO was determined by HPLC combined with a turbidimetry method (Lu et al., 2005b). In vitro release of coumarin-6 from Tf-PO in PBS (pH 4 or 7.4) and in rat plasma was characterized as previously described (Pang et al., 2008). The released samples were analyzed by HPLC (Angilent 1200) with a fluorescence detector at an excitation wavelength of 465 nm and an emission wavelength of 502 nm (Lu et al., 2005b). Samples were kept away from light throughout the experimental procedure.

2.3. Cellular uptake of coumarin-6 loaded polymersomes

2.3.1. Fluorescent microscopy of polymersomes uptake by bEnd.3 cells

The bEnd.3 cells were seeded onto a polylysine-coated glass cover slip at a density of 10^4 cells per cm^2 and were incubated at 37 °C for 24 h. After a 30-min incubation in DMEM, cells were treated with coumarin-6-loaded Tf-PO or PO suspensions (100 μg/mL in DMEM) for 0.25, 0.5 and 2 h at 37 °C, respectively. At the end of the experiment, the cells were washed three times

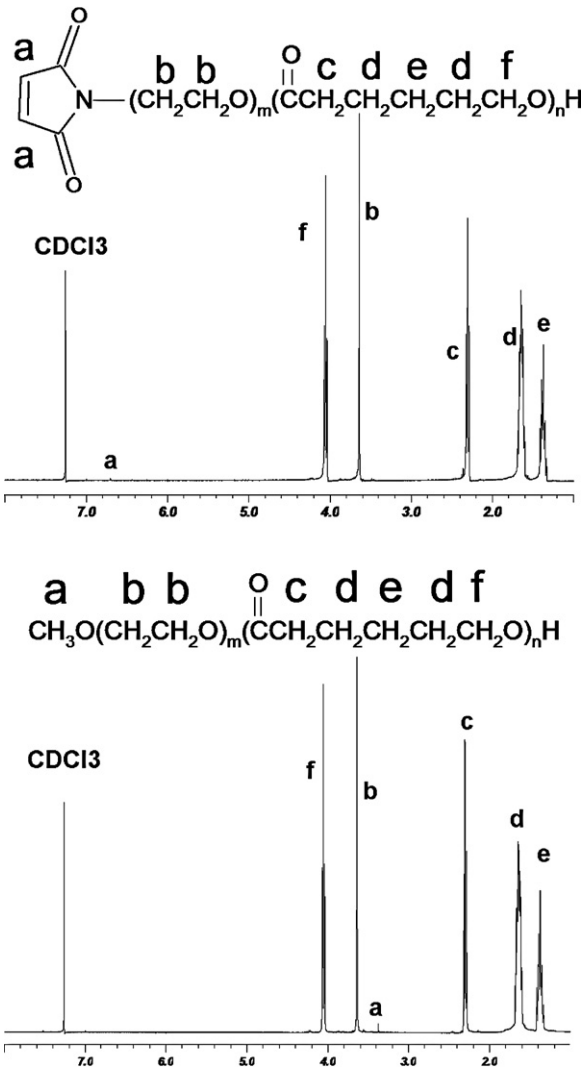

Fig. 1. ^{1}H NMR spectra of Maleimide-PEG3.4k–PCL15k (A) and MPEG3k–PCL15k (B) in CDCl3.

with PBS and fixed by 4% paraformaldehyde for 15 min. After being washed with PBS 3 times, the cells were mounted in Dako fluorescent mounting medium and observed under a fluorescent microscope (Olympus, Japan).

2.3.2. Quantitative determination of cellular uptake of coumarin-6 loaded polymersomes

To investigate the effect of different inhibitors on cellular uptake of Tf conjugated polymersomes, bEnd.3 cells were seeded onto a 24-well plate at a density of 10^5 cells per well and were incubated at 37 °C for 24 h. After a 30-min incubation in DMEM, the cells were treated with 100 μg/mL of coumarin-6-loaded Tf-PO and with various inhibitors for 60 min: DMEM (control), Tf (0.5 mg/mL), 0.1% (w/w) sodium azide, 20 μmol/L phenylarsinoxide (PheAso), 10 μg/mL chlorpromazine, 5 μg/mL Brefeldin A, 100 nmol/L monensin or 10 μg/mL filipin (Drin et al., 2003). At the end of the incubation period, the polymersomes suspension was removed, and the cells were washed three times with ice-cold PBS, subsequently with acid buffer (consisting of 120 mM NaCl, 20 mM sodium barbital, and 20 mM sodium acetate, pH 3) at 4 °C for 5 min, and again with ice-cold PBS. Afterward, the cells were solubilized with 0.4 mL of 1% Triton X-100 at 4 °C overnight, and 25 μL of the cell lysate from each well was sampled to determine the total cell protein content using the BCA protein assay. The rest of the cell lysate was used for extraction and HPLC determination of courmarin-6 (Lu et al., 2005b). The standard curve for polymersomes was constructed by suspending polymersomes in varying concentrations (5–200 μg/mL) in 1% Triton X-100 followed by the same extraction and HPLC determination process as the previous samples. Polymersome uptake was presented as the percent uptake of the control.

To evaluate the effect of temperature on cellular uptake, the cells were treated with the same process as described above except that the cells were incubated with 100 μg/mL of coumarin-6-loaded Tf-PO or PO at 4 °C and 37 °C for 1 h, respectively. The uptake index (UI) was expressed as polymersomes (μg)/cellular protein (mg).

To study the effects of incubation time on polymersome uptake, the cells were treated with the same process as described above except that the cells were incubated with 100 μg/mL of coumarin-6-loaded Tf-PO or PO at 37 °C for 0.25, 0.5, 1 and 2 h, respectively. The uptake index (UI) was expressed as polymersomes (μg)/cellular protein (mg).

Table 1
Particle size and zeta potential of PO and Tf-PO loaded with or without coumarin-6 ($n = 3$).

Vesicle	Mean size (mean ± SD, nm)	Zeta potential (mV)[a]
PO	95.2 ± 3.5	−20.2 ± 0.7
Tf-PO	99.1 ± 5.5	−20.5 ± 0.8
Courmarin-6-loaded PO	98.2 ± 6.7	−20.3 ± 0.5
Courmarin-6-loaded Tf-PO	101.4 ± 5.9	−19.9 ± 0.5

[a] Measured in NaCl solution (10^{-3} M).

2.4. In vitro cytotoxicity of Tf-PO

The bEnd.3 cells were seeded onto a 96-well plate at a density of 10^4 cells per well and incubated for 24 h. Afterward the cells were incubated with PO and Tf-PO samples in DMEM with a series of concentrations for 4 h at 37 °C. Eight wells treated only with DMEM were prepared as controls. After exposure to polymersomes, the cytotoxicity of these formulations was assayed by the MTT method (Lu et al., 2005a).

2.5. Brain delivery of Tf-PO

2.5.1. Qualitative studies

To verify the brain delivery property of Tf-PO, the experiment was performed as previously described (Hu et al., 2009; Lu et al., 2005b). Briefly, coumarin-6-labeled Tf-PO or PO was injected into rat tail veins at a dose of 50 mg/kg. Thirty minutes later, the animals were anaesthetized, and the heart was perfused with 100 mL of saline followed by 200 mL of 4% paraformaldehyde. Afterwards, the brain was removed and fixed in 4% paraformaldehyde overnight. Samples measuring 0.5 cm in thickness of the coronal section post optic chiasma were collected and placed in 15% sucrose PBS solution for 12 h followed by 30% sucrose overnight. The samples were embedded in Tissue Tek® O.C.T. compound (Sakura, USA) and frozen at −70 °C. The frozen sections of 5 μm thickness were prepared with a cryotome Cryostat (Leica, CM 1900, Germany), and were stained with 1 μg/mL DAPI for 10 min at room temperature. The sections were washed with PBS 3 times, mounted in fluorescent mounting medium and examined under the fluorescence microscope (Olympus, Japan).

2.5.2. Quantitative studies

Animal experiments were performed as previously described (Pang et al., 2008). In brief, rats were anesthetized with chloral hydrate. Then, coumarin-6-labeled Tf-PO and PO were injected into the left femoral vein at a dose of 10 mg/kg. Blood samples were collected via a cannula implanted in the left

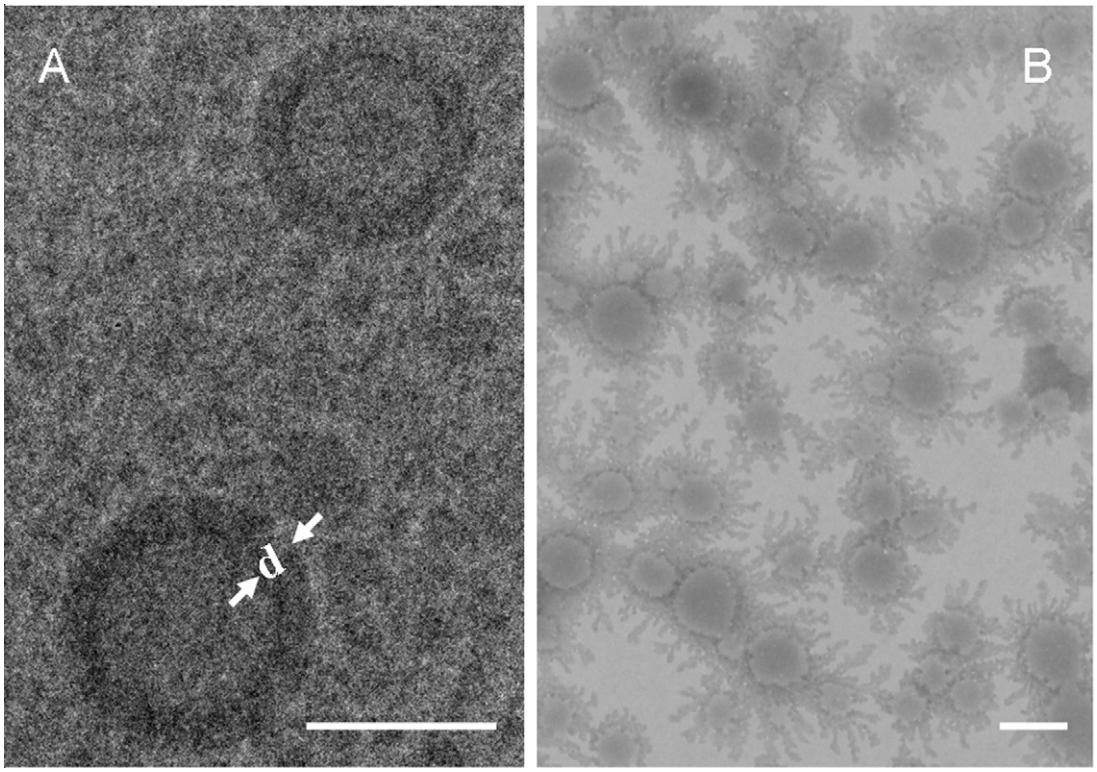

Fig. 2. (A) Cryo-TEM images of polymersomes in water (bar 100 nm). The hydrophobic cores of polycaprolactone are the darker areas. (B) TEM images of Tf-PO negatively stained with 1% uranyl acetate solution (bar 100 nm).

femoral artery at 0.25, 1, 2, 5, 15, 30, 60 and 120 min following i.v. injection. The blood volume was replaced with an equal volume of saline. At 120 min, the animals were decapitated, and the brain and other major organs including the liver, spleen, heart, lung and kidneys were collected followed by quick washing with cold saline to remove surface blood. The tissue samples and blood samples were spiked with the internal standard coumarin-7 and were subjected to n-hexane extraction for HPLC analysis as previously described (Lu et al., 2007).

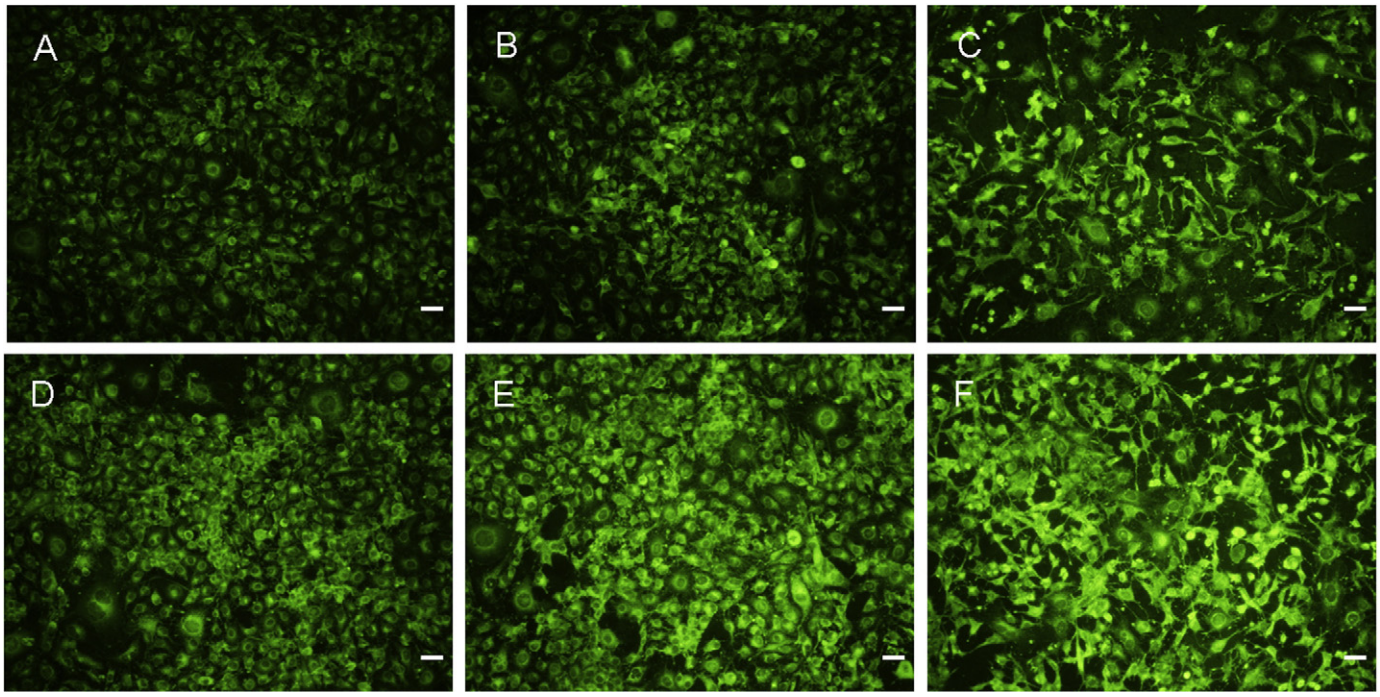

Fig. 3. Fluorescence imaging of bEnd.3 uptake of 100 μg/mL polymersomes (upper row) and Tf-PO (lower row) at 37 °C incubation for 0.25 h (A and D), 0.5 h (B and E) and 2 h (C and F), respectively. The magnification bar is 25 μm.

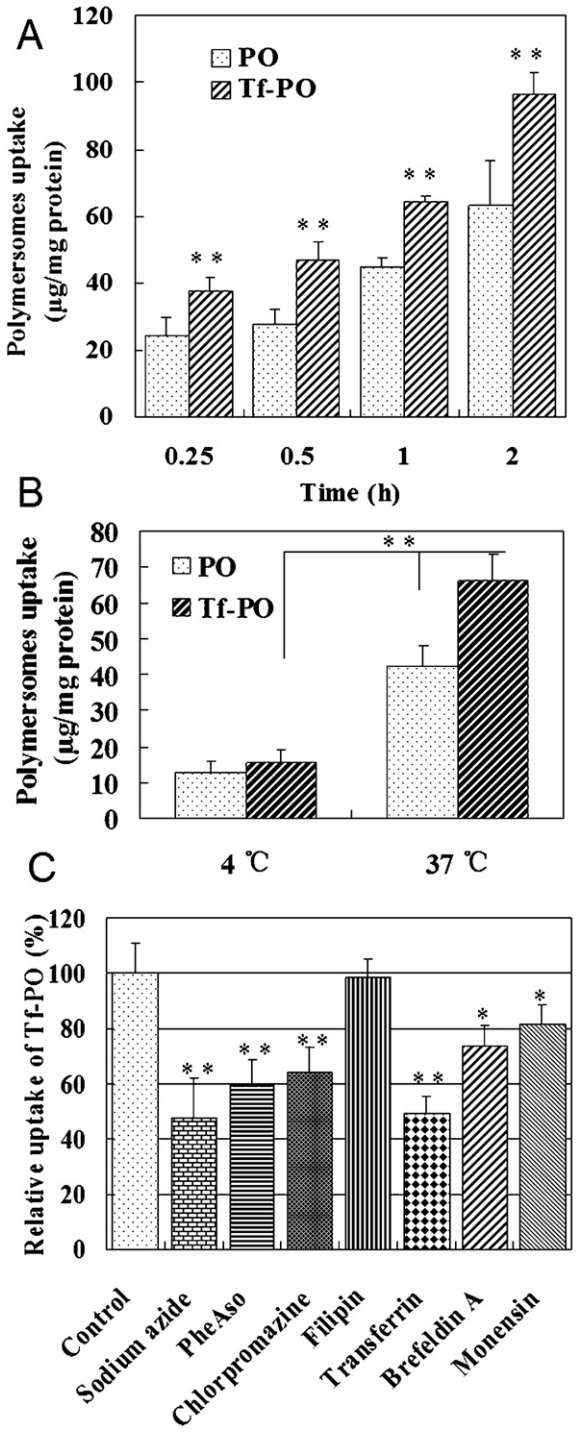

Fig. 4. Cell uptake of polyersomes with different time at 37 °C (A), at different incubation temperatures (B) or in the presence of various inhibitors of endocytosis (C). The bEnd.3 cells were incubated with 100 μg/mL of PO or Tf-PO samples. Data represented the mean ± SD ($n = 4$). Statistically significant difference by Student's t-test when compared to the corresponding value of control. (A) $^{**}p < 0.01$ vs PO; (B) $^{**}p < 0.01$ vs Tf-PO at 37 °C; (C) $^{*}p < 0.05$, $^{**}p < 0.01$ vs control.

Using a nonlinear regression, the plasma data was fitted to a biexponential equation:

$$A(t) = A_1 e^{-k_1 t} + A_2 e^{-k_2 t},$$

where $A(t)$ was %ID per mL of plasma (%ID, percentage of injected dose) (Kang et al., 1994). Pharmacokinetic parameters, such as plasma clearance (Cl) and steady-state volume of distribution

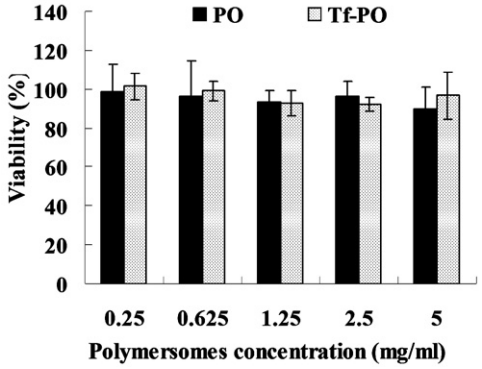

Fig. 5. In vitro cytotoxicity of PO, Tf-PO against bEnd.3 cells with a series of concentrations from 0.25 to 5 mg/mL. Data represented the mean ± SD ($n = 4$).

(Vss) were calculated from A_1, A_2, k_1, and k_2. The area under the blood concentration curve (AUC_{0-t}) was calculated using a noncompartmental data analysis of the blood concentrations. The brain permeability surface area (PS) product was determined as described elsewhere (Huwyler et al., 1996). Brain uptake was expressed as %ID per g of tissue and calculated as:

$$\%ID/g(t) = PS \times AUC_{0-t}.$$

3. Results and discussion

3.1. Copolymer synthesis

Two block copolymers, MPEG3k–PCL15k and Maleimide-PEG3.4k–PCL15k, were synthesized with molecular weights of 15,200 and 15,300 Da, respectively, as determined by ^{1}H NMR (Fig. 1). The typical ^{1}H NMR spectra and chemical shifts of these copolymers were in good agreement with previously published data on PEG–PCL copolymers (Yuan et al., 2000) and on maleimide functions (Olivier et al., 2002). For Maleimide-PEG–PCL, the existing peak for maleimide protons proved that the maleimide function was mostly preserved in the final product. GPC measurements demonstrated that the polydispersity index of MPEG3k–PCL15k and Maleimide-PEG3.4k–PCL15k were 1.18 and 1.27, respectively.

3.2. Characterization of transferrin conjugated polymersomes

Cryo-TEM results revealed that a blend of MPEG3k–PCL15k and Maleimide-PEG3.4k–PCL15k spontaneously assembled into polymersomes with a diameter of approximately 100 nm (Fig. 2A). The hydrophobic core of the polymersome membrane provided the contrast, and the membrane thickness has a measured width of about 18 nm. These self-assembled bilayers were considerably thicker than any previously studied lipid system, indicating they may be electromechanically tough, have low permeability and good stability (Discher et al., 1999). TEM examination demonstrated that polymersomes had an average diameter of approximately 90 nm (Fig. 2B), and the conjugation with Tf did not change their vesicle-like shape. The vesicle size and zeta potential of polymersomes measured by DLS were shown in Table 1. The average diameter of unconjugated polymersomes was around 95 nm, and the vesicle size was slightly increased to approximately 100 nm after transferrin conjugation or coumarin-6 incorporation. It has been shown that the optimal size for polymersomes is 100 nm for improving the PK parameters (Alexis et al., 2008), and that a similar size is advantageous for endocytosis by brain capillary endothelial cells (Huwyler et al., 1996; Massignani et al., 2009). No significant difference in vesicle size was observed between unloaded Tf-PO and

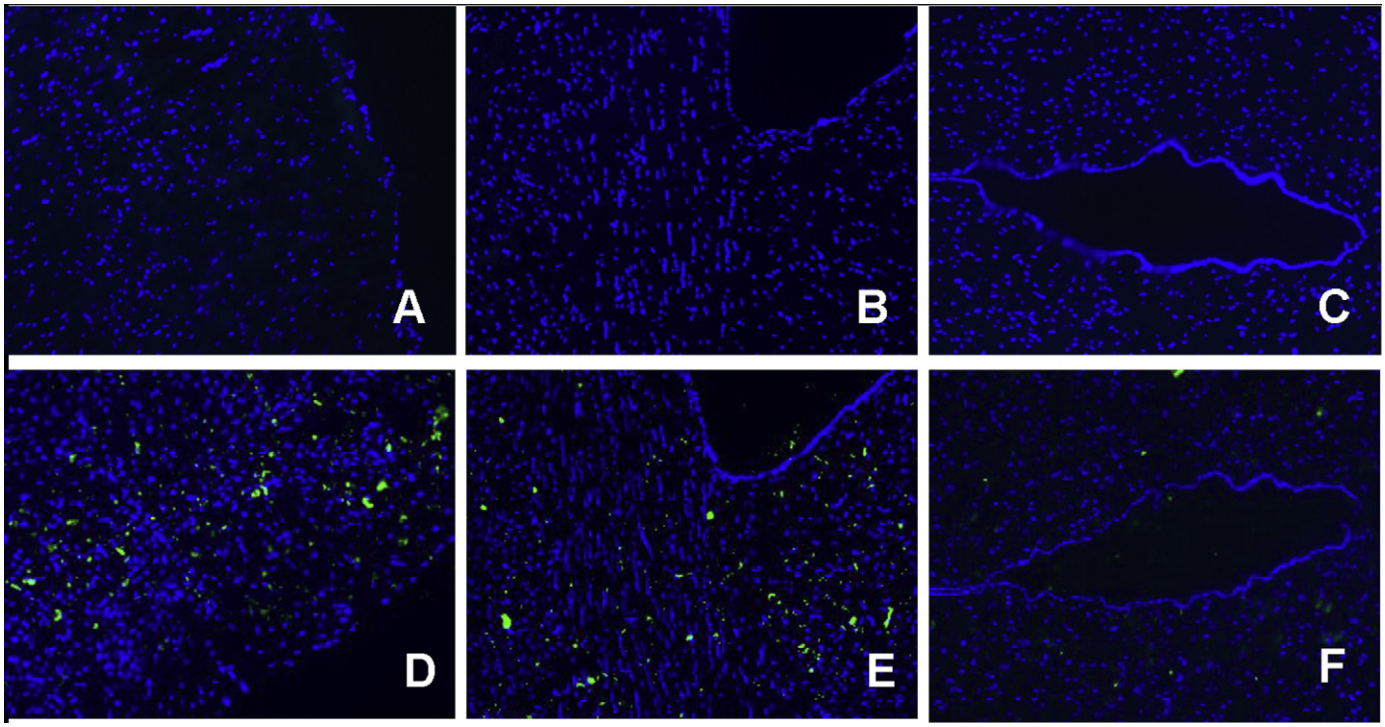

Fig. 6. Distribution of coumarin-6 labeled PO (upper row) and Tf-PO (lower row) in cerebral cortex (A and D), the periventricular region of lateral ventricle (B and E) and the third ventricle (C and F) was visualized using the FITC filter 30 min after i.v. injection of polymersomes at a dose of 50 mg/kg (green). The cell nuclei were stained with 1 μg/mL DAPI visualized using UV filter (blue). (For interpretation of the references to color in this figure legend, the reader is referred to the web version of the article.)

those loaded with coumarin-6, indicating that the incorporation of coumarin-6 did not influence the vesicle size. The zeta potential values of polymersomes, Tf-PO and coumarin-6 loaded Tf-PO in 0.001 M NaCl solution (pH 7.0) were all approximately −20 mV. There was no significant difference in the zeta potential value between PO and Tf-PO loaded with or without coumarin-6, indicating that Tf conjugation and coumarin-6 incorporation did not influence the zeta potential value. There were 37.3 ± 3.5 transferrin molecules on the surface of each Tf-PO, which was a reasonable density for brain targeting (Huang et al., 2007; Huwyler et al., 1996).

As an accurate fluorescent probe, coumarin-6 was usually encapsulated into nanocarriers to trace the behavior of nanocarriers in vitro and in vivo (Davda and Labhasetwar, 2002; Gao et al., 2006). In this study, the DLE of coumarin-6 loaded Tf-PO and PO were 0.81% and 0.83%, respectively. This amount of coumarin-6 proved to be enough for qualitative and quantitative study both in vitro and in vivo (Davda and Labhasetwar, 2002; Lu et al., 2007). In vitro release tests demonstrated that the accumulated percentage of coumarin-6 released from Tf-PO in pH 4.0, 7.4 PBS and rat plasma for 60 h were approximately 0.49%, 0.43% and 2.77%, respectively. The low leakage property of coumarin-6 from polymersomes indicated that the fluorescence signal detected in the cells, blood or organ samples was mainly attributed to the coumarin-6 encapsulated into the polymersomes. Therefore, coumarin-6 could be a suitable fluorescent probe for the polymersomes' behavior in vitro and in vivo.

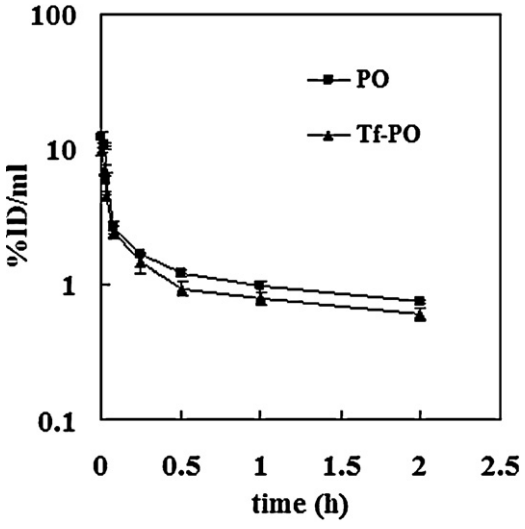

Fig. 7. %ID/mL of plasma of polymersomes is plotted vs various times after intravenous injection. Data are means ± SD of $n = 4$ rats/point.

A major concern with using nanocarriers for brain delivery is neurotoxicity; however, biodegradable nanocarriers are generally safe when used for brain delivery. In our previous report, it was also shown wheat germ agglutinin conjugated biodegradable nanoparticles exerted little toxicity on the brain after intranasal delivery to the brain (Liu et al., 2011). In this study, block copolymer PEG–PCL was selected for preparing polymersomes due to its biodegradability. Unlike our previous reported "biodegradable polymersomes", which were formed from blending bioinert polymers and biodegradable components (Gao et al., 2010), PEG–PCL polymersomes promise to be fully biodegradable, leaving no potentially toxic byproducts upon their degradation (Ghoroghchian et al., 2006). It has been previously shown that PEO2k–PCL12k and PEG3k–PCL15.8k, which have a relatively low hydrophilic volume fraction ($f = 0.15$ and 0.17, respectively) can form vesicles by a film hydration method (Ghoroghchian et al., 2006; Pang et al., 2010). However, the hydration process needed high temperatures for a long time, which might induce degradation of the polyesters block and inactivation of the maleimide group. In this study, a nanoprecipitation method was applied to prepare PEG–PCL polymersomes under mild conditions. It was found that PEG–PCL with

Table 2
Pharmacokinetic parameters and brain delivery of polymersomes after i.v. injection.

Group	AUC_{ss} (%ID*h/mL)	AUC_{0-t} (%ID*h/mL)	Cl (mL/h/kg)	MRT (h)	PS (μL/h/g)	%ID/g brain
PO	4.57 ± 0.75	2.65 ± 0.28	99 ± 15	2.44 ± 0.65	18.6 ± 1.7	0.049 ± 0.005
Tf-PO	2.66 ± 0.62*	2.16 ± 0.15*	172 ± 36**	1.23 ± 0.41*	52.6 ± 7.2**	0.113 ± 0.018**

Values were mean ± SD, $n = 4$. Statistically significant difference by Student's t-test when compared to the corresponding value of control.
* $p < 0.05$ vs PO.
** $p < 0.01$ vs PO.

an f of 0.18 self-assembled into vesicles. This was not in agreement with the previous reports that amphiphilic diblock polymers self-assembling into polymersomes generally possess an f between 0.20 and 0.42 (Discher et al., 2007). These results indicate that both the preparation method and the hydrophilic volume fraction of copolymers might affect the formation of polymersomes.

3.3. Cellular uptake of polymersomes

As an immortalized mouse brain endothelial cell line, bEnd.3 cells exhibit endothelial properties, blood–brain barrier characteristics and amenability to numerous molecular interventions. They are typically chosen as a simple BBB model to study the brain delivery properties of nanocarriers in vitro (Brown et al., 2007; Hu et al., 2009). In this study, fluorescence imaging revealed that bEnd.3 cellular uptake of Tf-PO was higher than that of PO at the same time point (Fig. 3). The cellular uptake of both Tf-PO and PO increased with time, showing a time-dependent pattern. Quantitative determination results also proved that Tf-PO accumulated within the cells at a faster rate and to a larger extent than PO (Fig. 4A). After a 2-h incubation period, the cellular uptake index of Tf-PO was 1.53-fold higher than that of unconjugated PO. These results agreed well with our previous report (Gao et al., 2010). Moreover, polymersome uptake by bEnd.3 cells showed a temperature or energy dependent pattern. As shown in Fig. 4B and C, the uptake index of both Tf-PO and PO at 37 °C was much higher than at 4 °C. Energy depletion by sodium azide significantly decreased the cellular uptake of Tf-PO. The cellular internalization pathway of Tf-PO was characterized by adding a pharmacological inhibitor of clathrin-mediated endocytosis, chlorpromazine, and an inhibitor of caveolae-mediated endocytosis, filipin, into the mediums, respectively. It was evidenced that chlorpromazine significantly decreased the cellular uptake of Tf-PO but that filipin did not have any effect, indicating that clathrin but not caveolae was involved in the endocytosis process of Tf-PO (Fig. 4C). In addition, both excess free transferrin and PheAso, inhibitors of endocytosis greatly reduced the polymersome uptake, suggesting that uptake of Tf-PO was subject to receptor-mediated endocytosis. The Golgi apparatus and lysosomes have important roles in both intracellular cargo transport and disposition (Gabor et al., 2002; Jiang et al., 2006). In this study, both BFA, which disrupts the Golgi apparatus and intracellular trafficking, and monensin, a lysosome inhibitor, significantly reduced the uptake of Tf-PO (Fig. 3A), confirming that both the Golgi apparatus and lysosomes are involved in intracellular transport of Tf-PO. All of these results suggest that Tf-PO interacts with the BBB in a specific manner that facilitates their endocytosis.

Many studies have demonstrated that transferrin increases brain delivery of nanocarriers via receptor-mediated transcytosis; however, little is known about the cellular internalization pathway of transferrin modified nanocarriers. In contrast to previous reports that a caveolae endocytosis pathway is preferentially involved in the cellular uptake of transferrin conjugated nanoparticles (Tf-NPs) (Chang et al., 2009), Tf-PO uptake by bEnd.3 cells occurred via a clathrin-mediated endocytosis, and both the Golgi apparatus and the lysosome had important effects on intracellular transport of Tf-PO. Interestingly, Tf was also shown to cross the BBB via caveolae or clathrin-mediated transcytosis in different in vitro BBB models (Candela et al., 2008; Simionescu et al., 2002; Visser et al., 2004). These results suggested that the characteristics of Tf-PO uptake by different cells might be rather different, and rational BBB models should be applied to study the internalization pathways of nanocarriers. More details about intracellular internalization by colocalization with endocytosis markers such as clathrin-specific antibodies, caveolin-1-specific antibodies and cholera toxin B for caveolae (Sahay et al., 2008) are still in need of further investigation.

3.4. In vitro cytotoxicity of Tf-PO

As shown in Fig. 5, Tf-PO and PO displayed little toxicity against bEnd.3 cells. Even at the highest concentration (5 mg/mL), the cellular viability was always above 89%. There were no significant differences in cellular viability between the PO and Tf-PO groups. These results indicate that biodegradable Tf-PO has good safety.

3.5. Brain delivery of Tf-PO

The microscopic examination of coronal sections of the rat brain after i.v. injection of fluorescent polymersomes showed that coumarin-6 labeled Tf-PO localized in the cerebral cortex, the periventricular region of the lateral ventricle and the third ventricle, whereas PO exhibited little distribution (Fig. 6). These results suggest that Tf-PO is an effective carrier for brain delivery.

3.6. Pharmacokinetics and brain delivery of coumarin-6 loaded Tf-PO

Pharmacokinetics experiments were performed in SD rats in order to quantitatively investigate the brain delivery properties of Tf-PO. As shown in Fig. 7, after i.v. injection of polymersomes at a dose of 10 mg/kg, the blood clearance of both Tf-PO and PO occurred in a biexponential manner (Fig. 7). From the data in Fig. 7, pharmacokinetic parameters and brain uptake of polymersomes were calculated (Table 2). Both Tf-PO and PO showed long circulation properties; however, Tf conjugation significantly increased the plasma clearance and decreased the MRT. Although Tf conjugation significantly decreased the AUC_{0-t} of polymersomes, the PS product for Tf-PO was increased to 2.8-fold that of PO. The brain uptake for Tf-PO at 2 h was 0.11%ID/g, which increased by 2.3-fold when compared with PO. All these results indicated that Tf-PO might be a promising carrier for brain delivery and may have good potential to deliver therapeutic agents to the CNS for the treatment of neurodegenerative diseases.

4. Conclusion

In this paper, a novel brain delivery nanocarrier, transferrin conjugated biodegradable polymersomes (Tf-PO), was exploited for efficient brain drug delivery, and its cellular internalization mechanisms were investigated. It was evidenced that Tf-PO uptake by bEnd.3 cells occurred mainly through a clathrin-mediated, energy-dependent endocytosis and that both the Golgi apparatus and lysosomes are involved in intracellular transport of Tf-PO. Fluo-

rescent microscopy of brain coronal sections revealed that after i.v. injection more Tf-PO than PO accumulated in the brain. In addition, the brain delivery results proved that the blood–brain barrier (BBB) permeability surface area product (PS) and percentage of injected dose per gram of brain (%ID/g brain) for Tf-PO were increased 2.8-fold and 2.3-fold when compared with those of PO, respectively. These results indicated that Tf-PO is a promising brain delivery carrier.

Acknowledgements

This work was supported by the National Basic Research Program of China (973 Program) 2007CB935800, the National Science and Technology Major Project 2009ZX09310-006, the National Natural Science Foundation of China (30762544), and the young teacher's initiative foundation of the School of Pharmacy, Fudan University.

References

Alexis, F., Pridgen, E., Molnar, L.K., Farokhzad, O.C., 2008. Factors affecting the clearance and biodistribution of polymeric nanoparticles. Mol. Pharm. 5, 505–515.
Bermudez, H., Brannan, A.K., Hammer, D.A., Bates, F.S., Discher, D.E., 2002. Molecular weight dependence of polymersome membrane structure, elasticity, and stability. Macromolecules 35, 8203–8208.
Brown, R.C., Morris, A.P., O'Neil, R.G., 2007. Tight junction protein expression and barrier properties of immortalized mouse brain microvessel endothelial cells. Brain Res. 1130, 17–30.
Candela, P., Gosselet, F., Miller, F., Buee-Scherrer, V., Torpier, G., Cecchelli, R., Fenart, L., 2008. Physiological pathway for low-density lipoproteins across the blood–brain barrier: transcytosis through brain capillary endothelial cells in vitro. Endothelium 15, 254–264.
Cerritelli, S., Velluto, D., Hubbell, J.A., 2007. PEG-SS-PPS: reduction-sensitive disulfide block copolymer vesicles for intracellular drug delivery. Biomacromolecules 8, 1966–1972.
Chang, J., Jallouli, Y., Kroubi, M., Yuan, X.B., Feng, W., Kang, C.S., Pu, P.Y., Betbeder, D., 2009. Characterization of endocytosis of transferrin-coated PLGA nanoparticles by the blood–brain barrier. Int. J. Pharm. 379, 285–292.
Chen, W., Meng, F., Cheng, R., Zhong, Z., 2010. pH-Sensitive degradable polymersomes for triggered release of anticancer drugs: a comparative study with micelles. J. Control. Release 142, 40–46.
Davda, J., Labhasetwar, V., 2002. Characterization of nanoparticle uptake by endothelial cells. Int. J. Pharm. 233, 51–59.
de Boer, A.G., Gaillard, P.J., 2007. Drug targeting to the brain. Annu. Rev. Pharmacol. Toxicol. 47, 323–355.
de Boer, A.G., van der Sandt, I.C., Gaillard, P.J., 2003. The role of drug transporters at the blood–brain barrier. Annu. Rev. Pharmacol. Toxicol. 43, 629–656.
Discher, B.M., Won, Y.Y., Ege, D.S., Lee, J.C., Bates, F.S., Discher, D.E., Hammer, D.A., 1999. Polymersomes: tough vesicles made from diblock copolymers. Science 284, 1143–1146.
Discher, D.E., Eisenberg, A., 2002. Polymer vesicles. Science 297, 967–973.
Discher, D.E., Ortiz, V., Srinivas, G., Klein, M.L., Kim, Y., Christian, D., Cai, S., Photos, P., Ahmed, F., 2007. Emerging applications of polymersomes in delivery: from molecular dynamics to shrinkage of tumors. Prog. Polym. Sci. 32, 838–857.
Drin, G., Cottin, S., Blanc, E., Rees, A.R., Temsamani, J., 2003. Studies on the internalization mechanism of cationic cell-penetrating peptides. J. Biol. Chem. 278, 31192–31201.
Du, J., O'Reilly, R.K., 2009. Advances and challenges in smart and functional polymer vesicles. Soft Matter 5, 3544–3561.
Gabor, F., Schwarzbauer, A., Wirth, M., 2002. Lectin-mediated drug delivery: binding and uptake of BSA-WGA conjugates using the Caco-2 model. Int. J. Pharm. 237, 227–239.
Gan, C.W., Feng, S.S., 2010. Transferrin-conjugated nanoparticles of poly(lactide)-D-alpha-tocopheryl polyethylene glycol succinate diblock copolymer for targeted drug delivery across the blood–brain barrier. Biomaterials 31, 7748–7757.
Gao, H.L., Pang, Z.Q., Fan, L., Hu, K.L., Wu, B.X., Jiang, X.G., 2010. Effect of lactoferrin- and transferrin-conjugated polymersomes in brain targeting: in vitro and in vivo evaluations. Acta Pharmacol. Sin. 31, 237–243.
Gao, X., Tao, W., Lu, W., Zhang, Q., Zhang, Y., Jiang, X., Fu, S., 2006. Lectin-conjugated PEG-PLA nanoparticles: preparation and brain delivery after intranasal administration. Biomaterials 27, 3482–3490.
Gatter, K.C., Brown, G., Trowbridge, I.S., Woolston, R.E., Mason, D.Y., 1983. Transferrin receptors in human tissues: their distribution and possible clinical relevance. J. Clin. Pathol. 36, 539–545.
Ghoroghchian, P.P., Li, G., Levine, D.H., Davis, K.P., Bates, F.S., Hammer, D.A., Therien, M.J., 2006. Bioresorbable vesicles formed through spontaneous self-assembly of amphiphilic poly(ethylene oxide)-block-polycaprolactone. Macromolecules 39, 1673–1675.
Gupta, Y., Jain, A., Jain, S.K., 2007. Transferrin-conjugated solid lipid nanoparticles for enhanced delivery of quinine dihydrochloride to the brain. J. Pharm. Pharmacol. 59, 935–940.
He, C., Sun, J., Deng, C., Zhao, T., Deng, M., Chen, X., Jing, X., 2004. Study of the synthesis, crystallization, and morphology of poly(ethylene glycol)–poly(epsilon-caprolactone) diblock copolymers. Biomacromolecules 5, 2042–2047.
Hu, K., Li, J., Shen, Y., Lu, W., Gao, X., Zhang, Q., Jiang, X., 2009. Lactoferrin-conjugated PEG-PLA nanoparticles with improved brain delivery: in vitro and in vivo evaluations. J. Control. Release 134, 55–61.
Huang, R.Q., Qu, Y.H., Ke, W.L., Zhu, J.H., Pei, Y.Y., Jiang, C., 2007. Efficient gene delivery targeted to the brain using a transferrin-conjugated polyethyleneglycol-modified polyamidoamine dendrimer. FASEB J. 21, 1117–1125.
Huwyler, J., Wu, D., Pardridge, W.M., 1996. Brain drug delivery of small molecules using immunoliposomes. Proc. Natl. Acad. Sci. U.S.A. 93, 14164–14169.
Jefferies, W.A., Brandon, M.R., Hunt, S.V., Williams, A.F., Gatter, K.C., Mason, D.Y., 1984. Transferrin receptor on endothelium of brain capillaries. Nature 312, 162–163.
Jiang, S., Rhee, S.W., Gleeson, P.A., Storrie, B., 2006. Capacity of the Golgi apparatus for cargo transport prior to complete assembly. Mol. Biol. Cell 17, 4105–4117.
Jones, A.R., Shusta, E.V., 2007. Blood–brain barrier transport of therapeutics via receptor-mediation. Pharm Res. 24, 1759–1771.
Kang, Y.S., Bickel, U., Pardridge, W.M., 1994. Pharmacokinetics and saturable blood–brain barrier transport of biotin bound to a conjugate of avidin and a monoclonal antibody to the transferrin receptor. Drug Metab. Dispos. 22, 99–105.
Ke, W., Shao, K., Huang, R., Han, L., Liu, Y., Li, J., Kuang, Y., Ye, L., Lou, J., Jiang, C., 2009. Gene delivery targeted to the brain using an Angiopep-conjugated polyethyleneglycol-modified polyamidoamine dendrimer. Biomaterials 30, 6976–6985.
Liu, G., Ma, S., Li, S., Cheng, R., Meng, F., Liu, H., Zhong, Z., 2010. The highly efficient delivery of exogenous proteins into cells mediated by biodegradable chimaeric polymersomes. Biomaterials 31, 7575–7585.
Liu, L., Guo, K., Lu, J., Venkatraman, S.S., Luo, D., Ng, K.C., Ling, E.A., Moochhala, S., Yang, Y.Y., 2008. Biologically active core/shell nanoparticles self-assembled from cholesterol-terminated PEG-TAT for drug delivery across the blood–brain barrier. Biomaterials 29, 1509–1517.
Liu, Q., Shao, X., Chen, J., Shen, Y., Feng, C., Gao, X., Zhao, Y., Li, J., Zhang, Q., Jiang, X., 2011. In vivo toxicity and immunogenicity of wheat germ agglutinin conjugated poly(ethylene glycol)–poly(lactic acid) nanoparticles for intranasal delivery to the brain. Toxicol. Appl. Pharmacol. 251, 79–84.
Lu, W., Tan, Y.Z., Hu, K.L., Jiang, X.G., 2005a. Cationic albumin conjugated pegylated nanoparticle with its transcytosis ability and little toxicity against blood–brain barrier. Int. J. Pharm. 295, 247–260.
Lu, W., Wan, J., She, Z., Jiang, X., 2007. Brain delivery property and accelerated blood clearance of cationic albumin conjugated pegylated nanoparticle. J. Control. Release 118, 38–53.
Lu, W., Zhang, Y., Tan, Y.Z., Hu, K.L., Jiang, X.G., Fu, S.K., 2005b. Cationic albumin-conjugated pegylated nanoparticles as novel drug carrier for brain delivery. J. Control. Release 107, 428–448.
Mabrouk, E., Cuvelier, D., Brochard-Wyart, F., Nassoy, P., Li, M.H., 2009. Bursting of sensitive polymersomes induced by curling. Proc. Natl. Acad. Sci. U.S.A. 106, 7294–7298.
Massignani, M., LoPresti, C., Blanazs, A., Madsen, J., Armes, S.P., Lewis, A.L., Battaglia, G., 2009. Controlling cellular uptake by surface chemistry, size, and surface topology at the nanoscale. Small 5, 2424–2432.
Meng, F., Engbers, G.H., Feijen, J., 2005. Biodegradable polymersomes as a basis for artificial cells: encapsulation, release and targeting. J. Control. Release 101, 187–198.
Meng, F., Hiemstra, C., Engbers, G.H.M., Feijen, J., 2003. Biodegradable polymersomes. Macromolecules 36, 3004–3006.
Meng, F., Zhong, Z., Feijen, J., 2009. Stimuli-responsive polymersomes for programmed drug delivery. Biomacromolecules 10, 197–209.
Olivier, J.C., Huertas, R., Lee, H.J., Calon, F., Pardridge, W.M., 2002. Synthesis of pegylated immunonanoparticles. Pharm. Res. 19, 1137–1143.
Pang, Z., Feng, L., Hua, R., Chen, J., Gao, H., Pan, S., Jiang, X., Zhang, P., 2010. Lactoferrin-conjugated biodegradable polymersome holding doxorubicin and tetrandrine for chemotherapy of glioma rats. Mol. Pharm. 7, 1995–2000.
Pang, Z., Lu, W., Gao, H., Hu, K., Chen, J., Zhang, C., Gao, X., Jiang, X., Zhu, C., 2008. Preparation and brain delivery property of biodegradable polymersomes conjugated with OX26. J. Control. Release 128, 120–127.
Pardridge, W.M., 2002. Drug and gene targeting to the brain with molecular Trojan horses. Nat. Rev. Drug Discov. 1, 131–139.
Pardridge, W.M., 2007. Blood–brain barrier delivery. Drug Discov. Today 12, 54–61.
Qian, Z., Li, H., Sun, H., Ho, K., 2002. Targeted drug delivery via the transferrin receptor-mediated endocytosis pathway. Pharmacol. Rev. 54, 561–587.
Qin, S., Geng, Y., Discher, D.E., Yang, S., 2006. Temperature-controlled assembly and release from polymer vesicles of poly(ethylene oxide)-block-poly(*N*-isopropylacrylamide). Adv. Mater. 18, 2905–2909.
Ren, W.H., Chang, J., Yan, C.H., Qian, X.M., Long, L.X., He, B., Yuan, X.B., Kang, C.S., Betbeder, D., Sheng, J., et al., 2010. Development of transferrin functionalized poly(ethylene glycol)/poly(lactic acid) amphiphilic block copolymeric micelles as a potential delivery system targeting brain glioma. J. Mater. Sci. Mater. Med. 21, 2673–2681.
Sahay, G., Batrakova, E.V., Kabanov, A.V., 2008. Different internalization pathways of polymeric micelles and unimers and their effects on vesicular transport. Bioconjug. Chem. 19, 2023–2029.

Simionescu, M., Gafencu, A., Antohe, F., 2002. Transcytosis of plasma macromolecules in endothelial cells: a cell biological survey. Microsc. Res. Tech. 57, 269–288.
Visser, C.C., Stevanovic, S., Heleen Voorwinden, L., Gaillard, P.J., Crommelin, D.J., Danhof, M., De Boer, A.G., 2004. Validation of the transferrin receptor for drug targeting to brain capillary endothelial cells in vitro. J. Drug Target. 12, 145–150.
Ying, X., Wen, H., Lu, W.L., Du, J., Guo, J., Tian, W., Men, Y., Zhang, Y., Li, R.J., Yang, T.Y., et al., 2009. Dual-targeting daunorubicin liposomes improve the therapeutic efficacy of brain glioma in animals. J. Control. Release 141, 183–192.
Yuan, M., Wang, Y., Li, X., Xiong, C., Deng, X., 2000. Polymerization of lactides and lactones. 10. Synthesis, characterization, and application of amino-terminated poly(ethylene glycol)-co-poly(ε-caprolactone) block copolymer. Macromolecules 33, 1613–1617.
Zhou, W., Meng, F., Engbers, G.H., Feijen, J., 2006. Biodegradable polymersomes for targeted ultrasound imaging. J. Control. Release 116, e62–e64.